Molecular Crystals and Liquid Crystals

Publication details, including instructions for authors and subscription information:
http://www.tandfonline.com/loi/gmcl20

Director Fields Around Spherical and Cylindrical Micro Particles in a Liquid Crystal Host

H. Matthias [a] & H.-S. Kitzerow [a]

[a] Faculty of Science, University of Paderborn, Paderborn, Germany

Version of record first published: 05 Oct 2009

To cite this article: H. Matthias & H.-S. Kitzerow (2009): Director Fields Around Spherical and Cylindrical Micro Particles in a Liquid Crystal Host, Molecular Crystals and Liquid Crystals, 508:1, 127/[489]-136/[498]

To link to this article: http://dx.doi.org/10.1080/15421400903060300

Mol. Cryst. Liq. Cryst., Vol. 508, pp. 127/[489]–136/[498], 2009

ISSN: 1542-1406 print/1563-5287 online
DOI: 10.1080/15421400903060300

Taylor & Francis
Taylor & Francis Group

Director Fields Around Spherical and Cylindrical Micro Particles in a Liquid Crystal Host

H. Matthias and H.-S. Kitzerow
Faculty of Science, University of Paderborn, Paderborn, Germany

Director fields around spherical and cylindrical micro particles embedded in a uniformly aligned nematic liquid crystal are investigated by means of fluorescence confocal polarizing microscopy. Both dipolar configurations (point-like defects) and quadrupolar configurations (ring-like defect lines) are observed for spherical particles. However, only defect lines appear in the vicinity of particles with cylindrical shape. In contrast to previous predictions for sphero-cylinders, the defect lines around the cylindrical particles studied here seem to be pinned at the cylinder edges. The experimental results are in good agreement with numerical simulations.

Keywords: liquid crystals; micro particles; suspensions; topology

1. INTRODUCTION

Investigations on the director fields of liquid crystals in complex geometries [1] become increasingly important in connection with non-conventional displays and novel photonic applications. During the last decades, the development of polymer-dispersed liquid crystal displays, liquid crystalline gels and tunable photonic crystals have lead to extended research on the effects of confinement of liquid crystals to spherical, elliptical, cylindrical of more complex cavities [1–5]. However, the inverse problem, i. e. the effect of incorporation of small particles in a liquid crystal on the director field surrounding the particles is very important, as well. Since a long time, it is known that the surface of liquid crystals can be decorated by micron-sized droplets,

Financial support of this work by the European Science Foundation (EUROCORES, 05-SONS-FP-014) and the German Research Foundation (DFG, KI 411/14-1) is gratefully acknowledged.

Address correspondence to H.-S. Kitzerow, Universitat Paderborn, Dept. Chemie, Warburger Str. 100, Paderborn D33098, Germany. E-mail: kitzerow@chemie.upb.de

which form chains that visualize the local director [6,7]. The experiments by Poulin *et al.* [8] and their theoretical analysis [9–11] initiated more recent research. The possibility to arrange micron-sized particles by means of optical tweezers [12] and the analysis of the particle interactions have lead to additional knowledge on this problem. Increasing interest in anisotropic suspensions of nanoparticles can be expected to stimulate the field further. Today, the director configurations that appear when micron-sized spherical particles are embedded in a uniformly parallel oriented nematic liquid crystal are well explored. It is accepted that a particle with homeotropic surface anchoring corresponds to a hedgehog disclination. Its positive topological charge [7] needs to be compensated by a neighbouring disclination with negative topological charge. The latter might be a point-like defect ("dipole configuration") or a defect ring ("Saturn ring") surrounding the particle ("quadrupole configuration"), see Figure 1. The elastic energy of the liquid crystal causes the formation of particle chains parallel to the bulk director orientation in the case of dipole configurations, while it favors chains or arrays of particles oblique to the bulk director in the case of quadrupole configurations. In addition to spherical particles, suspensions of elongated particles were considered recently [13,14], but received limited attention, so far. In this study, the novel method of fluorescence confocal polarizing microscopy (FCPM) is tested for spherical particles and applied to study the

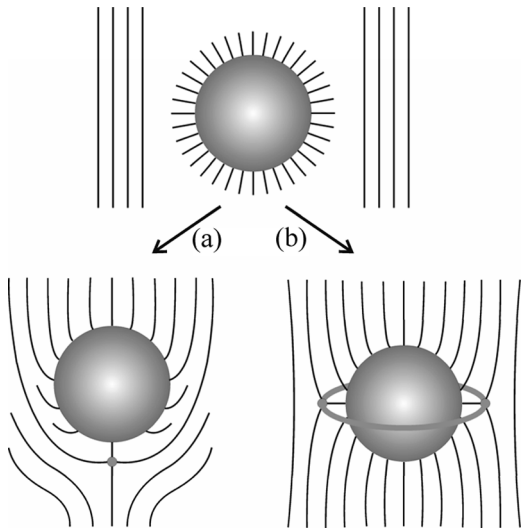

FIGURE 1 Topological defects around spherical micro particles.

director fields around glass cylinders immersed in a uniformly aligned nematic liquid crystal.

2. EXPERIMENTS AND NUMERICAL SIMULATIONS

In the experimental part of this study, the director fields of spherical and cylindrical particles suspended in the nematic liquid crystal MLC 6609 [Merck, $\Delta n = 0.0777$] were examined. As micro spheres, we used colloidal particles of different size. The smaller particles consist of silica with a diameter $D \approx 0.5\,\mu m$, the larger ones are melamin spheres with a diameter $D \approx 1.8\,\mu m$. In the case of anisotropic particles, silica rods with $D \approx 4\,\mu m$ and an aspect ratio of 1.5 to 4 were studied. In order to achieve homeotropic anchoring, we suspended the particles in a DMOAP/isopropanol solution and dried them subsequently. Aligned nematic director fields were obtained in cells consisting of PVA-coated and rubbed cover glasses. The small silica spheres were prepared in wedged cells with a 5 μm spacer on one and no spacer on the other side. This allows a variation of the cell thickness (Fig. 2). In the other cases, we used planar cells with a thickness of 10 μm.

To study the liquid crystalline director fields experimentally, we applied the FCPM method. FCPM uses a scanning laser beam focused on the sample, which is doped with a small amount (<0.1 weight%) of an anisometric fluorescent dye (BTBP in our case). The transition dipole moment of the dichroic dye is oriented along the local director of the liquid crystal host [15]. The incident laser beam (488 nm, Ar^+) as well as the emitted light pass a polarizer, which implies that the intensity of the detected light scales as $I \propto \cos^4\alpha$ for an angle α between the local director and the electric field vector of the polarized light. Since the fluorescence wavelength of BTBP peaks at $\lambda \approx 540\,nm$, the exciting and the fluorescence light can be effectively separated by a filter with an absorption edge at 510 nm.

From the variety of numerical methods available for modelling the director configurations we chose the Q-tensor method as described in Refs. [16,17]. Starting from the dynamic equation for the director,

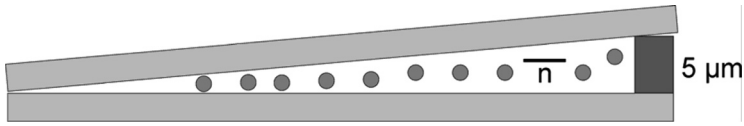

FIGURE 2 Wedge cell used to vary the distance of the aligning glass substrates continuously.

the following algorithm can be derived

$$Q_{jk}^{\tau+1} = Q_{jk}^{\tau} + \frac{\Delta t}{\gamma_1}[f_s]_{Q_{jk}}. \tag{1}$$

The functional derivative $[f_s]_{Qjk}$ is retained by integrating the free energy density over the simulated volume and applying the Euler-Lagrange method

$$\begin{aligned}[f_s]_{Q_{jk}} = &-\frac{2}{S^2}\left(-\frac{1}{12}K_{11}+\frac{1}{4}K_{22}+\frac{1}{12}K_{33}\right)Q_{jk,ll}\\ &-\frac{1}{S^2}(K_{11}-K_{22}-K_{33})Q_{jl,lk}+\frac{1}{S^2}K_{24}Q_{jl,lk}+\frac{1}{4S^3}(K_{33}-K_{11})\\ &\times\left(Q_{lm,j}Q_{lm,k}-Q_{lm,l}Q_{jk,m}-Q_{lm}Q_{jk,ml}-Q_{lm,m}Q_{jk,l}-Q_{lm}Q_{jk,lm}\right)\\ &+\frac{2}{S^2}q_0K_{22}\varepsilon_{jlm}Q_{mk,l}\end{aligned} \tag{2}$$

Summation over repeated indices is assumed, and the definition of the Q-terms can be found in Ref. [17]. S is the scalar order parameter and the elastic coefficients K_{11}, K_{22}, K_{33}, and K_{24} describe the elastic energy due to splay, twist, bend and saddle-splay deformations, respectively.

In this study, computer programs based on the algorithm (2) were used in order to simulate the distorted nematic director fields surrounding the micro particles. The volume of a cell was discretized by $100 \times 63 \times 63$ grid points of constant mesh-size. The elasticity coefficients of MLC 6609 were estimated by the values of a typical nematic liquid crystal (5CB, [18]) as $K_{11} = 6.4$ pN, $K_{22} = 3$ pN, $K_{33} = 10$ pN. Starting from a randomly oriented isotropic phase, 10,000 iteration steps were performed.

3. RESULTS

Experimental FCPM images of spherical micro particles indicate two different director configurations (Figs. 3a and 3b, respectively). Both types of images exhibit two-fold symmetry with the symmetry axis approximately parallel to the bulk director orientation that is induced by rubbing. However, one type of images (Fig. 3a) indicates a rather prolate shape, the other type (Fig. 3b) a rather oblate shape of the distorted director region around the spherical particle. The first type (Fig. 3a) can be attributed to a dipolar director configuration, while comparison with numerical calculations (Fig. 4) indicates that the second type (Fig. 3b) corresponds to the quadrupolar director configuration.

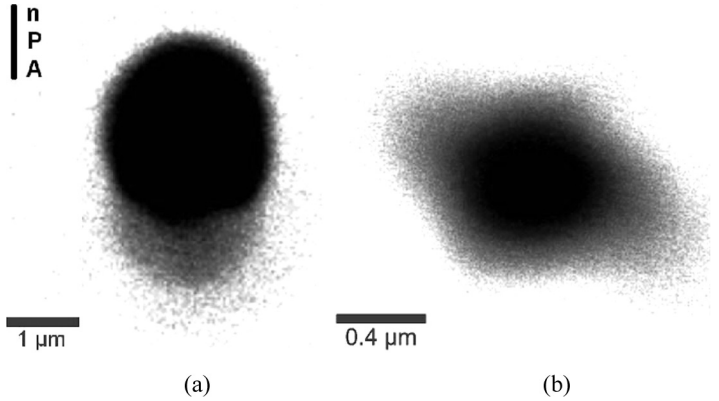

FIGURE 3 FCPM images of embedded melamin micro-spheres indicate the dipole configuration (a), silica particles exhibit a quadrupolar configuration (b). The director is designated by **n**, the orientation of the polarizer and analyzer by **P** and **A**, respectively.

It is interesting to note that the dipolar configuration appears for larger particles, while the quadrupolar configuration appears for smaller particles. This experimental result is in agreement with earlier analytical and numerical calculations. The latter predict a higher stability of the dipole configuration for micron sized particles, while the quadrupole configuration gains stability if the droplet size is reduced [19]. Unfortunately, the resolution of this method is not sufficient to judge whether the hyperbolic defect of the bipolar director field is really point-like or consists in fact of a ring with a diameter

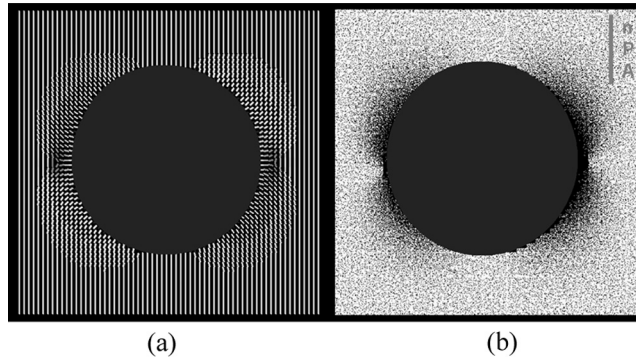

FIGURE 4 (a) Calculated director field of the quadrupolar structure and (b) the corresponding FCPM-pattern (spherical particle).

in the nm range [11]. However, the experimental FCPM pictures allow for a clear distinction between the two principal director configurations.

The shape of the silica rods that were dispersed in the nematic liquid crystal is quite different from the shape of the spherical particles described above. Nevertheless, the dispersion of rods with homeotropic anchoring in a uniformly oriented nematic environment is topological equivalent to the dispersion of spherical particles, i.e., the positive topological charge induced by the anchoring at the closed particle surface must be compensated by a negative topological charge in the nematic environment so that the entire sample remains topological uncharged. If such a rod is aligned approximately parallel to the bulk director (Fig. 5), the homeotropic alignment at its end faces is consistent with the uniform orientation of the environment. Consequently, the experimental image (Fig. 5a) indicates no director field deformation at the end faces. However, along the cylinder barrel, the director field is considerably deformed. This image is in good agreement with the numerical simulation of the director field and its calculated FCPM image (Fig. 5b). Although the diameter and the length of the suspended cylinder are considerably larger than the diameter of the spherical particle described above, there is no indication of an additional point defect in the vicinity of the cylindrical particle. Such a point defect would be expected in the case of the classical dipolar configuration. However, there is also no experimental proof for the appearance of a disclination ring (such as the Saturn ring in Fig. 3b). The simulation of the director field (Fig. 5c) indicates where the

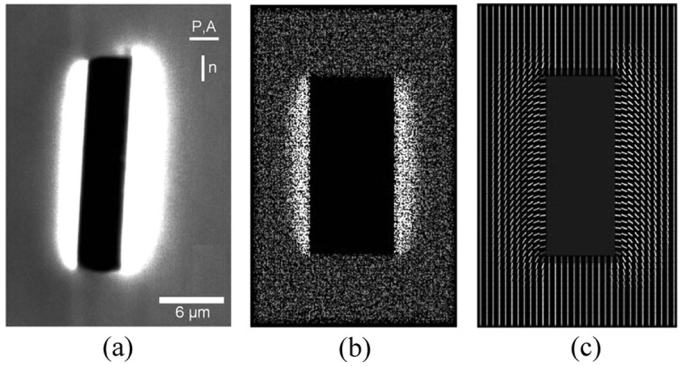

FIGURE 5 Silica rod parallel to the surrounding director field. (a) experimental PCPM image, (a) calculated FCPM image, (c) calculated director field with $a - 1/2$ defect ring at the left and $a + 1/2$ defect ring at the right edge of the rod.

negative topological charge is hidden: The planar projection of the director field (Fig. 5c) shows two defects with the disclination strength [7] $s = -1/2$ at the periphery of one cylinder head. Because of the cylindrical symmetry it can be concluded that a disclination ring appears close to the cylinder, which – unlike the Saturn ring around a spherical particle - is not located in the center of the suspended particle but pinned at one end of the cylinder. This finding is reasonable, since the sharp edges of the cylinders require an elastic deformation of the director anyway. On one end, this deformation may be continuous, but at the other end it coincides with a singularity of the director field.

If a cylindrical particle with homeotropic surface anchoring is aligned with its axis perpendicular to the director, the FCPM images (Fig. 6) look similar, although the geometry is slightly different from the situation described above. Again, no point-like disclination can be seen in the vicinity of the particle, which indicates the probable existence of a ring-like line disclination with the disclination strength $s = -1/2$ in the plane perpendicular to the bulk director. This situation is energetically not very favorable since the length of the disclination line increases with increasing length of the cylinder. However, the

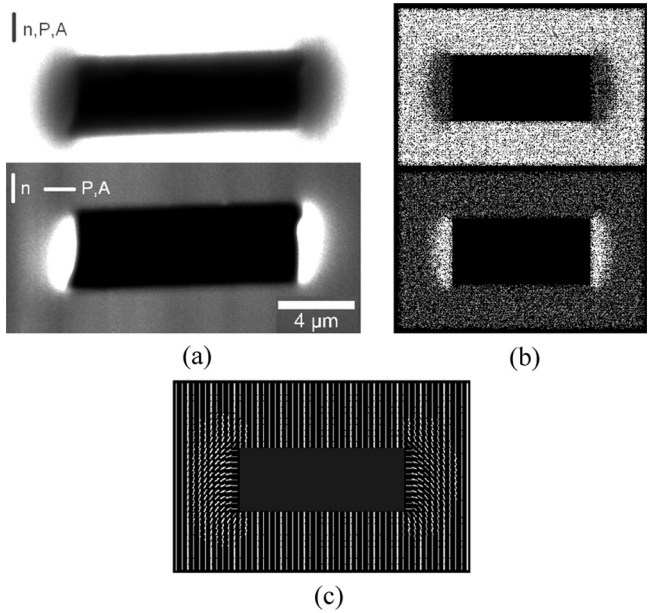

FIGURE 6 FCPM texture of a silica rod aligned perpendicular to the surrounding director.

appearance of a disclination line along the cylinder can obviously not be avoided: In the limit of an infinitely long cylinder, the director field depends only on the two spatial coordinates that are perpendicular to the cylinder axis. Clearly, in this essentially two-dimensional system it is obvious that there must exist at least one line-like disclination parallel to the cylinder in order to satisfy the boundary conditions.

4. CONCLUSIONS

In conclusion, the present investigation shows that FCPM is a useful tool in order to investigate the topology of the director field around micro-particles embedded in a liquid crystal. Although the resolution

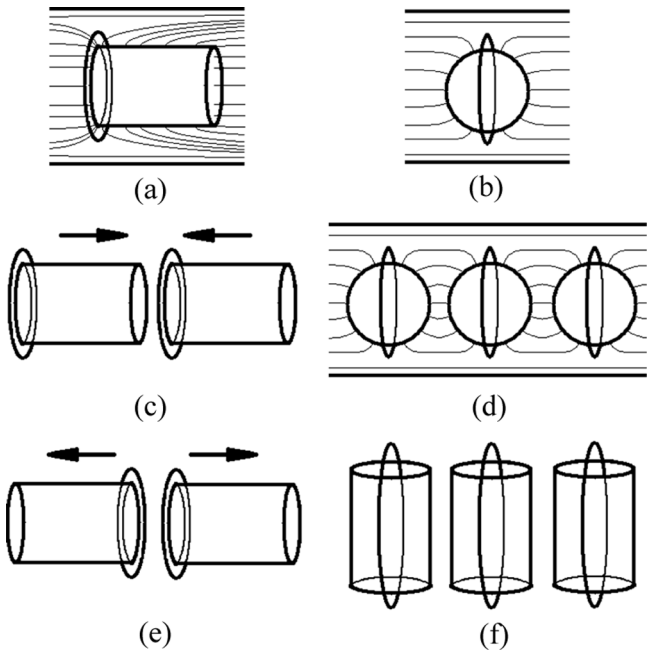

FIGURE 7 Director fields around cylindrical micro particles (a, b) and expected consequences for the particle aggregation (c–f). Thin lines in parts (a) and (b) indicate the director alignment, the thick line around the cylinder corresponds to the respective disclination ring with $s = -1/2$. (a) Cylindrical particle aligned along the surrounding director. (b) Cylindrical particle aligned perpendicular to the surrounding director. (c, e) Expected attraction (c) or repulsion (e), depending on the location of the disclination ring. (d, f) Expected aggregation of cylinders aligned perpendicular to the surrounding director: (d) side-view, (f) top-view.

of this method is limited (to $> 200\,\text{nm}$), it allows to identify point- and ring-like disclinations in the director field. Our experiments confirm the known director configurations around spherical particles and their relative stability depending on the particle size. In addition, the experiments on cylindrical particles reveal a slightly different behavior. Point-like disclinations as in the dipolar configuration (Fig. 1a) were never observed in the case of cylindrical particles. Thus, topological considerations indicate that there must be disclination rings in the latter case. This is confirmed by director field simulations. For parallel bulk alignment and homeotropic anchoring at the particles surface, these rings appear in a plane perpendicular to the bulk director. In contrast to spherical particles, the shape of the disclination ring depends on the orientation of the cylinder axis. If the latter is parallel to the bulk director, the disclination line has a circular shape and is found to be pinned on one end of the cylinder (Fig. 7a). However, the disclination loop is likely to consist of two straight $s = -1/2$ lines that are connected at the cylinder ends, if the cylinder axis is perpendicular to the bulk director (Fig. 7b). It is interesting to note that these differences imply a different symmetry. In the first case (Fig. 7a), the director field has a polar axis along the cylinder, while the latter case (Fig. 7b) resembles the quadrupolar type of symmetry. These differences imply also a dependence of the aggregation behavior of cylindrical particles on their orientation relative to the bulk director. For example, cylinders surrounded by a polar director field may attract (Fig. 7c) or repel each other (Fig. 7e), depending on their polar axes. In the case of favorable alignment, they may be expected to form chains along the cylinder axis. In contrast, the cylinders surrounded by a director field with non-polar symmetry can be expected to prefer the formation of side-on aggregates (Fig. 7d,f) rather than long chains. The investigation of these expectations will be the subject of further studies.

REFERENCES

[1] (1996). *Liquid Crystals in Complex Geometries Formed by Polymer and Porous Networks*, Crawford, G. P. & Zumer, S. (Eds.), Taylor & Francis: London.

[2] Drzaic, P. S. (1995). *Liquid Crystal Dispersions*, World Scientific: Singapore.

[3] Kitzerow, H.-S. (1994). Polymer-dispersed liquid crystals – from the nematic curvilinear aligned phase to ferroelectric films. *Liquid Crystals*, *16*, 1–31.

[4] Pierron, J., Tournier-Lasserve, V., Sopena, P., Boudet, A., Sixou, P., & Mitov, M. (1995). Three-dimensional microstructure of a polymer-dispersed liquid crystal observed by transmission electron microscopy. *J. Phys. II France*, *5*, 1635–1647.

[5] Kitzerow, H.-S., Lorenz, A., & Matthias, H. (2007). Tuneable photonic crystals obtained by liquid crystal infiltration. *Phys. Stat. Sol. (a)*, *204*(11), 3754–3767.

[6] Cladis, P. E., Kléman, M., & Piéranski, P. (1971). Sur une nouvelle méthode de décoration de la phase mésomorphe du p-méthoxybenzylidène p-butylaniline (MBBA). *C. R. Acad. Sc. Paris*, *273*, Série B, 275–277.
[7] de Gennes, P.-G. (1974). *The Physics of Liquid Crystals*, Clarendon Press: Oxford.
[8] Poulin, P., Stark, H., Lubensky, T. C., & Weitz, D. A. (1997). Novel colloidal interactions in anisotropic fluids. *Science*, *275*, 1770–1773.
[9] Ruhwandl, R. W. & Terentjev, E. M. (1997). Long-range forces and aggregation of colloid particles in a nematic liquid crystal. *Phys. Rev. E*, *55*, 2958–2961.
[10] Lubensky, T. C., Pettey, D., Currier, N., & Stark, H. (1998). Topological defects and interactions in nematic emulsions. *Phys. Rev. E*, *57*, 610–625.
[11] Fukuda, J., Yoneya, M., & Yokoyama, H. (2004). Nematic liquid crystal around a spherical particle: Investigation of the defect structure and its stability using adaptive mesh refinement. *Eur. Phys. J. E*, *13*, 87–98.
[12] Musevic, I., Skarabot, M., Tkalec, U., Ravnik, M., & Zumer, S. (2006). Two-dimensional nematic colloidal crystals self-assembled by topological defects. *Science*, *313*, 954–958.
[13] Andrienko, D., Allen, M. P., Skacej, G., & Zumer, S. (2002). Defect structures and torque on an elongated colloidal particle immersed in a liquid crystal host. *Phys. Rev. E*, *65*, 041702.
[14] Hung, F. R., Guzman, O., Gettelfinger, B. T., Abbott, N. L., & de Pablo, J. J. (2006). Anisotropic nanoparticles immersed in a nematic liquid crystal: Defect structures and potentials of mean force. *Phys. Rev. E*, *74*, 011711.
[15] Smalyukh, I. I., Shiyanovskii, S. V., & Lavrentovich, O. D. (2001). Three-dimensional imaging of orientational order by fluorescence confocal polarizing microscopy. *Chem. Phys. Lett.*, *336*, 88–96.
[16] Dickmann, S. (1994). *Numerische Berechnung von Feld und Molekülausrichtung in Flüssigkristallanzeigen*. Ph.D. thesis: University of Karlsruhe.
[17] Mori, H., Gartland, Jr., E. C., Kelly, J. R., & Bos, P. (1999). Multidimensional director modelling using the q tensor representation in a liquid crystal cell and its application to the π cell with patterned electrodes. *Jpn. J. Appl. Phys.*, *38*, 135–146.
[18] Blinov, L. M. & Chigrinov, V. G. (1994). *Electrooptic Effects in Liquid Crystal Materials*, Springer-Verlag: New York.
[19] Stark, H. (1999). *Physics of Inhomogeneous Nematic Liquid Crystals: Colloidal Dispersions and Multiple Scattering of Light*, Habilitation thesis: University of Stuttgart.